Received 13 January 2020; revised 6 March 2020; accepted 8 March 2020. Date of publication 23 March 2020;
date of current version 27 March 2020. The review of this paper was arranged by Editor C. C. McAndrew.

Digital Object Identifier 10.1109/JEDS.2020.2980759

1.4-kV Quasi-Vertical GaN Schottky Barrier Diode With Reverse *p-n* Junction Termination

RU XU, PENG CHEN, MENGHAN LIU, JING ZHOU, YUNFEI YANG, YIMENG LI, CHENG GE, HAOCHENG PENG, BIN LIU, DUNJUN CHEN, ZILI XIE, RONG ZHANG (Member, IEEE), AND YOUDOU ZHENG

Key Laboratory of Advanced Photonic and Electronic Materials, School of Electronic Science and Engineering, Nanjing University, Nanjing 210093, China

CORRESPONDING AUTHORS: P. CHEN and R. ZHANG (e-mail: pchen@nju.edu.cn; rzhang@nju.edu.cn)

This work was supported in part by the National High-Tech Research and Development Project under Grant 2015AA033305, in part by the Jiangsu Provincial Key Research and Development Program under Grant BK2015111, in part by the Collaborative Innovation Center of Solid State Lighting and Energy-Saving Electronics, in part by the Research Funds from NJU-Yangzhou Institute of Opto-Electronics, and in part by the Research and Development Funds from State Grid Shandong Electric Power Company and Electric Power Research Institute.

ABSTRACT In this paper, we demonstrate high-performance quasi-vertical GaN-on-Sapphire Schottky barrier diodes (SBD) with a reverse GaN *p-n* junction termination (RPN). The SBD has a current output of 1 kA/cm^2 at $V_F = 2.5$ V, a low V_{on} of 0.66 V $\pm$ 0.017 V, a low $R_{on,sp}$ of 1.4 mΩ·cm^2, current ON/OFF ratio of over 10^9 (-3 V$\sim$3 V). By introducing the RPN, the breakdown voltage can boost from 459 V to 1419 V, and power figure-of-merit (FOM) can reach 1438 MV/cm^2. It is shown that the presence of the RPN with a suitable anode recess depth can generate an electric field (EF) opposite to the built-in EF at the center of the second top *p-n* junction, which can decrease the EF peak intensity and make the electric field more uniformly distributed inside the device. Finally, the leakage current of the SBD is inhibited and the breakdown voltage is increased.

INDEX TERMS Vertical GaN-on-Sapphire Schottky barrier diode, reverse *p-n* GaN junction, breakdown voltage, power FOM.

I. INTRODUCTION

Group III nitrides represented by GaN have a wide range of applications in optoelectronics and power electronics, which is considered to be one of the most important semiconductor materials after silicon. Owing to its superior material properties such as high electric breakdown field, high-electron saturation velocity, and high mobility in a readily available heterojunction 2-dimensional electron gas (2-DEG) channel [1]–[3], GaN has been widely used in high frequency and power electronic devices. Power electronic devices are one of the fundamental components in almost all electronic manufacturing industries, including the field of consumer electronics, wireless communications and industrial control. Among all device types, Schottky barrier diodes (SBD) are the essential components in power conversion systems, such as switching power supply, frequency converter, driver and other circuits. In recent years, GaN vertical SBD devices have begun to receive more and more attention, especially for free-standing GaN vertical diodes [4]–[8]. However, the high cost and small size of GaN substrates are still the limiting factors for commercial free-standing GaN vertical power SBD devices. Therefore, GaN SBDs on silicon or sapphire substrates have begun to occupy the mainstream. It has been widely acknowledged that the excess leakage current arising from electric field (EF) crowding at the Schottky junction edge could lead to premature breakdown of the vertical SBDs [4], [6]. In order to improve the breakdown voltage, various edge terminal structures have been proposed, such as anode field plate (AFP), nitridation-based (negative ion implantation) termination and p-type junction termination (JBSD), etc., [7]–[20].

In this work, we proposed a new junction terminal structure. We propose a reverse p-n junction (RPN) terminal structure, which can further optimize the *EF* distribution in the SBD body, and use Silvaco-TCAD simulations and device performance to present the design principle and the function of the RPN structure.

II. DEVICE FABRICATION

The sample was grown on a 2-inch sapphire substrate by metal organic chemical vapor deposition (MOCVD).

This work is licensed under a Creative Commons Attribution 4.0 License. For more information, see https://creativecommons.org/licenses/by/4.0/

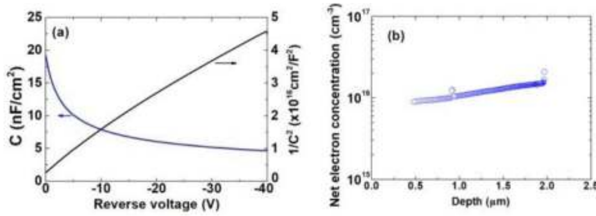

FIGURE 1. (a) C–V measurement on the n^-GaN drift layer at 100 kHz. (b) net electron concentration from the C–V measurement.

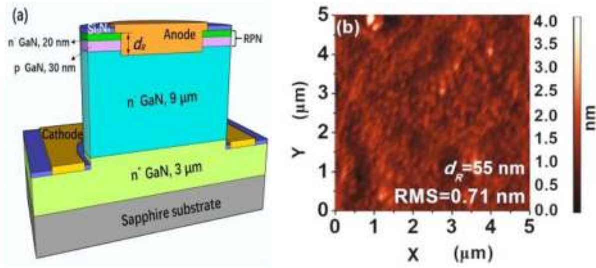

FIGURE 2. (a) Cross-section view of the quasi-vertical GaN SBD with reverse *p-n* junction termination (b) AFM image of the anode recessed surface with 55-nm recess depth in 5 μm by 5 μm area.

From the substrate, the device structure consists of a 3-μm n^+GaN with a doping concentration of $\sim 10^{19}$cm^{-3}, a 9-μm n^-GaN drift layer with a net electron concentration of $\sim 1.5\times 10^{16}$ cm^{-3}, which is obtained by capacitance–voltage (C–V) measurement as shown in Fig. 1. The C–V measurement (by Hg probe) on the entire epitaxial structure was performed by the epitaxy company. On the top of the drift layer, there are a 30-nm p-type GaN with a hole concentration of $\sim 4\times 10^{17}$ cm^{-3} by in-situ activation. The uppermost layer is 20-nm high resistance n^-GaN layer with a net electron concentration of $\sim 1\times 10^{15}$ cm^{-3}.

Fig. 2. (a) shows the cross-section of the SBDs. All SBDs feature a circular configuration with an effective width 130 μm, but with different d_R, which represents the anode recess depths from 0 nm (no recess) to 100 nm. Fabrication of the SBD commenced with growing a layer of SiO_2 as the cathode window etch mask by plasma-enhanced chemical vapor deposition (PECVD), and then cathode electrode region was defined by lithography. Next, the SiO_2 in the cathode region was etched by inductively coupled plasma (ICP) with an etching gas of C_4F_8.

In the second step, the cathode electrode region with a depth of 10 μm was etched into the n^+GaN layer by ICP with the etching gas consisting of the mixture of Cl_2/BCl_3. The rest of the SiO_2 mask was removed by buffered oxide etch (BOE) for 5 minutes.

In the third step, the anode recess was etched out with etch depth up to 100 nm by ICP. Then the sample was put into diluted KOH solution with a concentration of 0.1 mol/L for 15 minutes at 80°C in a water bath to remove the surface and sidewall damage caused by the ICP etching. The anode recessed surface with 55-nm recess depth was measured by an atomic force microscope (AFM) in 5 μm by 5 μm area. The AFM image is shown in Fig. 2(b), which gives a RMS of 0.71 nm. This result indicates a high quality of the Schottky surface and there is no etch pits observed on the surface.

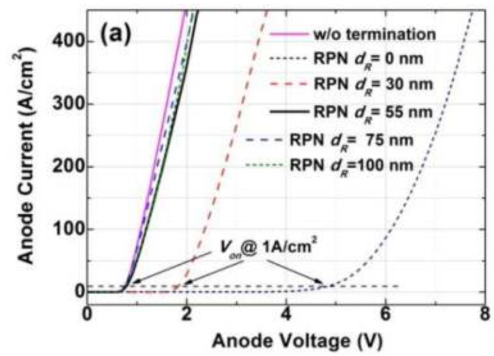

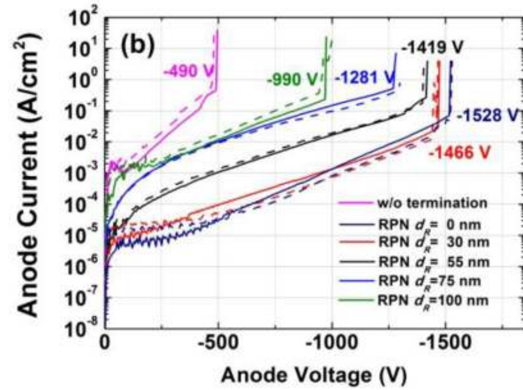

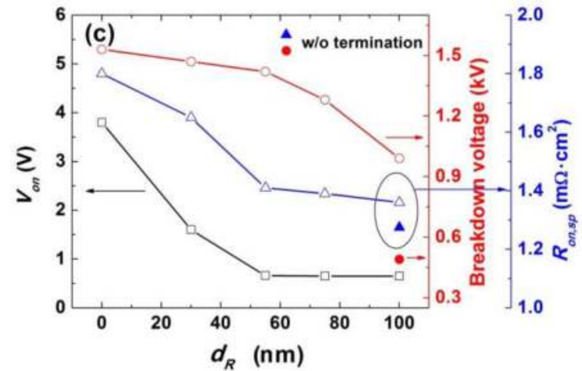

FIGURE 3. (a) Forward characteristics and (b) reverse characteristics for the SBD w/o termination and RPN SBDs with different anode recess depths d_R, (c) extracted V_{on} , BV and $R_{on,sp}$ changed with d_R. The V_{on} from the device without the termination is almost same to the one from the device with d_R of 100 nm.

The last step was evaporation of electrodes. First, we used Ti/Al/Ni/Au (30/150/30/100 nm) as the ohmic electrode and followed by rapid thermal annealing at 750°C for 30 s in a N_2 atmosphere. After that, the anode metal Pt/Au (50/300 nm) was evaporated on the recessed area with a 2-μm overlap on the RPN region. Finally, a 50-nm SiN_x passivation layer was deposited by using PECVD. For comparison, the SBD without the RPN termination was also fabricated.

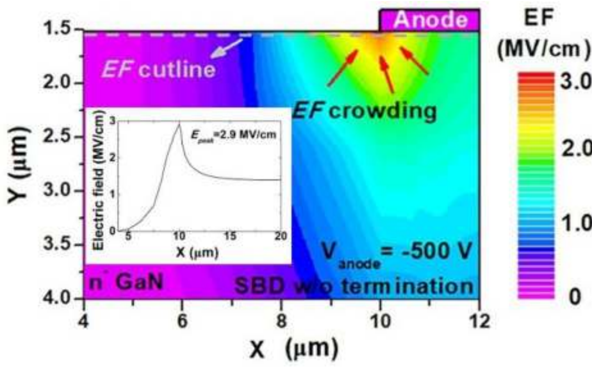

FIGURE 4. Electric field distribution of SBD w/o termination under a reverse bias of −500V, the insert is the extracted electric field near the surface.

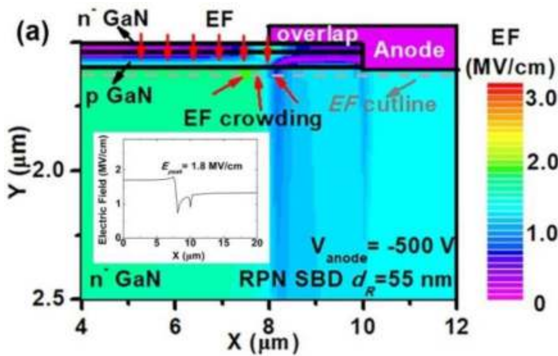

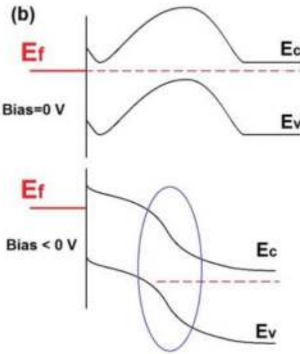

FIGURE 5. (a) EF distribution of the SBD with RPN termination under a reverse bias of −500V, (b) The schematic diagram of band bending.

III. RESULTS AND DISCUSSION

Different d_R has decisive effect on device performance. Fig. 3(a) and (b) is a comparison of the forward and reverse DC characteristics of the SBD under different d_R of 0 nm, 30 nm, 55 nm, 75 nm and 100 nm, respectively. A traditional SBD (without termination) sample also is shown. The V_{on} is defined as the voltage at a forward current of 1 A/cm^2, as shown in Fig. 3(a). The non-recessed diode has the highest V_{on} of 3.25 V, same as most reported GaN *p*-*n* junction diode [4]–[7]. With the deepening of the d_R till to 100 nm, V_{on} of the SBDs gradually decreases from about 3.25 V to about 0.66 V. The $R_{on,sp}$ of these diodes was calculated from *dV*/*dI* and normalized with respect to the effective

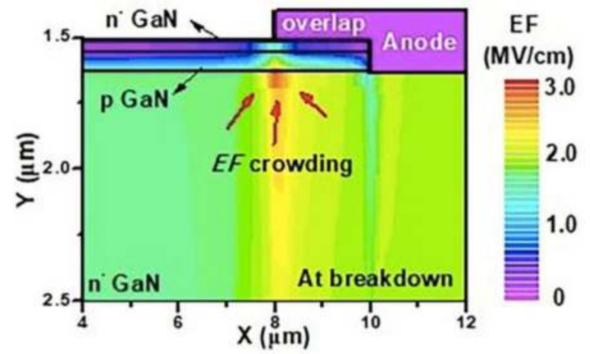

FIGURE 6. EF distribution of the SBD with RPN termination and d_R of 55 nm at the breakdown voltage.

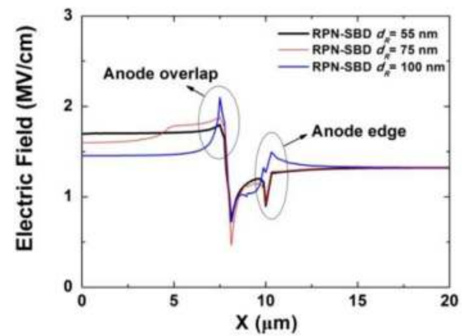

FIGURE 7. Extracted electric field distribution near the surface of the SBD devices with different d_R.

diode area. The $R_{on,sp}$ values vary between 1 ∼ 2 mΩ·cm^2, and decrease first and almost become flat for the d_R from 55 nm to 100 nm.

The reverse characteristics were shown in Fig. 3 (b), in which the dashed lines indicate the discrete range of each type of device. It can be seen that the SBDs with the RPN can greatly boost the breakdown voltage (BV) from 498 V to more than 1400 V, compared with the SBD without termination, indicating the effective function of the RPN. However, with the deepening of d_R, the breakdown voltage (BV) of the devices gradually decreases from more than 1500 V to 995 V. For a high-performance SBD, it is necessary to have high BV and low V_{on} at the same time. The relationship of V_{on} and BV depended on d_R was shown in Fig. 3. (c). It can be seen that the device with the d_R of 55nm has almost lowest V_{on} and higher BV. Therefore, considering both parameters, the SBD with the d_R of 55nm is the best one. In order to reveal the mechanism of RPN structure how to improve the breakdown voltage, a series of simulation studies were carried out by using Silvaco software.

The simulation results for the SBD without termination under a reverse bias of −500 V was shown in Fig. 4. Due to the edge curvature effect of Schottky junction, an electric field (EF) crowding at the anode edge can be seen with a peak value of 2.9 MV/cm.

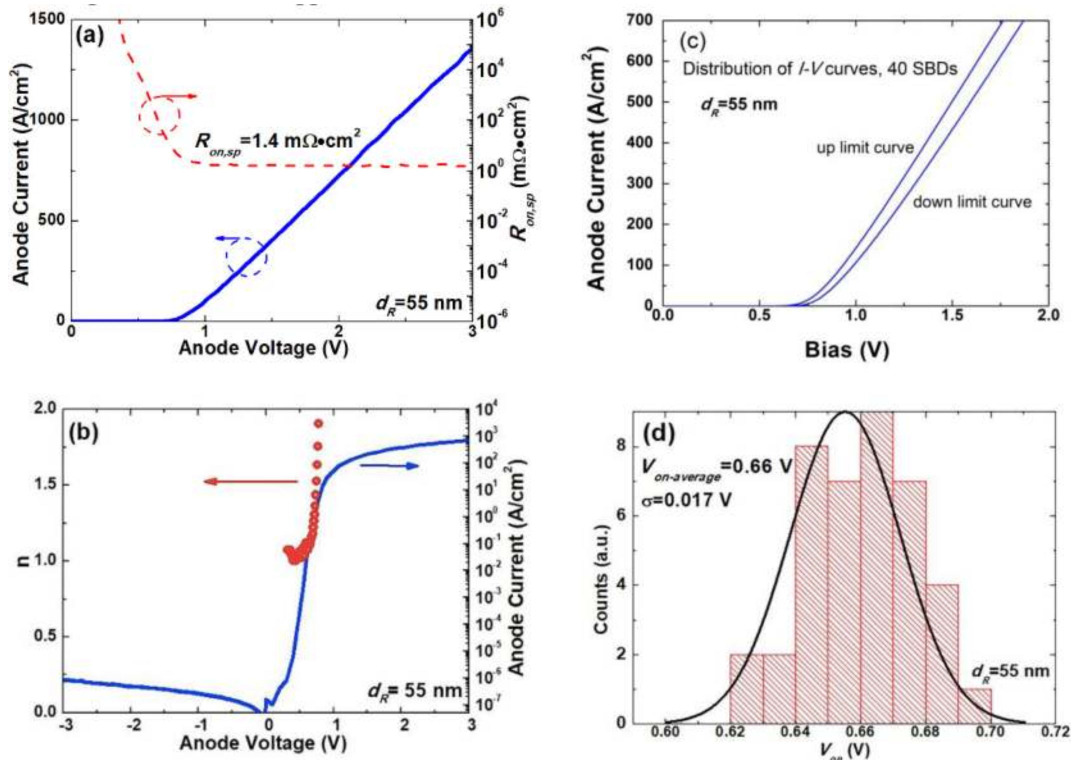

FIGURE 8. (a) Forward I–V curves of the RPN SBD and differential $R_{on,sp}$ (b) I-V curves of the RPN SBD from −3 to 3 V (c) Forward *I-V* curves of 40 RPN GaN SBDs (d) Distribution of the Von for the 40 RPN GaN SBDs.

The simulation results for the SBD with the RPN termination under the same reverse bias of −500 V was shown in Fig. 5 (a). The contact between anode and top n^-GaN is a Schottky contact. Compared to Fig. 4, the EF crowding at the anode edge almost disappeared, and the peak value of the EF has been greatly reduced to 1.8 MV/cm. It has been known that the uppermost layer is n^-GaN in the device structure, so the direction of the EF by the top *pn* junction is pointed to the substrate, while the direction of the EF by the Schottky contact is pointed to the top surface. Under a negative bias, the *pn* junction can still compensate part of the EF by the negative bias, resulting in a relative weak band bending near the top surface, which is equivalent to reducing the electric field strength in this area. The schematic diagram of band bending is shown in Fig. 5(b). From Fig. 5(b), it can be seen that the strongest band bending should located around the interface between the *p*-GaN and the drift layer, as indicated by the blue circle. If this situation continues, then the breakdown should occur inside the device.

Electric field distribution for the device with RPN structure and d_R of 55 nm at the breakdown voltages was also simulated, as shown in Fig. 6. It can be seen from this figure that the EF is greatly suppressed near the surface, and the peak position of the EF is indeed moved to the device, which is consistent with the discussion above. These results indicate that pushing the peak position away from the surface may help increase breakdown voltage of the device.

Although the RPN can effectively improve the BV of the SBD, above experimental results shows that with the increase of d_R, BV decreases gradually. The relationship between the BV and the d_R was investigated by simulation too, the bias is −500 V for all simulations. The electric field distribution near the surface of the SBDs with different d_R was shown in Fig. 7.

From Fig. 7, it can be seen that the highest EF always located under the anode overlap area, which is caused by the edge curvature effect. Please note that the top *pn* junction is about 50 nm thick. So the recess depth of 55 nm indicate the anode just contacts to the drift layer. But when the recess depth goes deeper, the peak of *EF* under the anode overlap will become more and more prominent, which could lead to pre-breakdown of the SBD. Thus, in order to make RPN work well, the d_R should be carefully controlled just to reach the top of the drift layer.

More features about the SBD device with d_R of 55 nm were analyzed. The *I-V* characteristics of the devices were shown in Fig. 8. (a) and (b). The RPN SBD with $d_R = 55$ nm exhibits a good turn-on characteristic with a V_{on} of 0.66V combined with a low leakage current below 10^{-6} A/cm^2, the current ON/OFF ratio can be more than 10^9 (based on −3 V to 3 V) at room temperature, the $R_{on,sp}$ is 1.4 mΩ·cm^2, which was calculated from *dV/dI*.

For Schottky forward characteristics, the I-V characteristic can be expressed by the theory of thermionic field

emission (TFE) as:

$$I = I_s \times \left[\exp\left(\frac{qV - I \times R_s}{nkT}\right) - 1\right] \quad (1)$$

where R_s is the series resistance, T is the absolute temperature, k is the Boltzmann constant, n is the ideal factor, and I_s is the reverse saturation current. n and $I_s$can be obtained by the slope and intercept of the ln *I-V* curve, respectively. Meanwhile, the Schottky barrier height φ_b can be expressed as:

$$\varphi_b = (kT/q) \times \ln\left(AA^* T^2/I_s\right) \quad (2)$$

where A is the effective area of the device and A^* is the Richardson constant, after calculation, the ideal factor n is 1.05 at 0.3∼0.6 V and Schottky barrier height, φ_b, is 0.68 ± 0.05 eV, respectively. But, with the increase of the bias over ∼0.7 V, the n factor increases sharply, which clear shows the damage that remains.

It should be noted that the forward current conduction mechanism is mainly based on thermionic emission mode, which matches equation (1). However, for the reverse characteristic, the depletion region will gradually grow. Therefore, equation (1) will not be applicable.

Fig. 8 (c) and (d) show the forward characteristics distributions of 40 RPN SBDs with d_R of 55 nm made from two different wafers. The average V_{on} of 40 SBDs is 0.66 V with a small standard deviation of 0.017 V, indicating high repeatability of our fabrication process. Overall, the device can present the power figure-of-merit (FOM) as high as 1438 MV/cm^2, demonstrating its great potential as power electronics application.

IV. CONCLUSION

In this work, we developed the high-performance quasi-vertical SBD by introducing the RPN terminal structure, which can optimize the internal *EF* distribution in the SBD device under reverse bias. These SBDs with the RPN terminal structure show V_{on} of 0.66 V, breakdown voltage of 1419 V, and $R_{on,sp}$ of 1.4 mΩ·cm^2. The power FOM is as high as 1438 MW/cm^2. Our results indicate that it is feasible to achieve high-performance GaN vertical SBDs with the reverse *p-n* junction termination.

ACKNOWLEDGMENT

The authors greatly appreciate Corenergy, Inc.'s support and collaboration on the growth of epitaxial wafer.

REFERENCES

[1] J. N. Gao *et al.*, "Low on-resistance GaN Schottky barrier diode with high V_{ON} uniformity using LPCVD Si_3N_4 compatible self-terminated, low damage anode recess technology," *IEEE Electron Device Lett.*, vol. 39, no. 6, pp. 859–862, Jun. 2018, doi: 10.1109/LED.2018.2830998.

[2] M. D. Zhu *et al.*, "1.9-kV AlGaN/GaN lateral Schottky barrier diodes on silicon," *IEEE Electron Device Lett.*, vol. 36, no. 4, pp. 375–377, Apr. 2015, doi: 10.1109/LED.2015.2404309.

[3] Y.-W. Lian, Y.-S. Lin, J.-M. Yang, C.-H. Cheng, and S. S. H. Hsu, "AlGaN/GaN Schottky barrier diodes on silicon substrates with selective Si diffusion for low onset voltage and high reverse blocking," *IEEE Electron Device Lett.*, vol. 34, no. 8, pp. 981–983, Aug. 2013, doi: 10.1109/LED.2013.2269475.

[4] H. Ohta *et al.*, "Vertical GaN p-n junction diodes with high breakdown voltages over 4 kV," *IEEE Electron Device Lett.*, vol. 36, no. 11, pp. 1180–1182, Nov. 2015, doi: 10.1109/LED.2015.2478907.

[5] I. C. Kizilyalli, T. Prunty, and O. Aktas, "4kV and 2.8mΩ·cm^2 vertical GaN p-n diodes with low leakage currents," *IEEE Electron Device Lett.*, vol. 36, no. 10, pp. 1073–1075, Oct. 2015, doi: 10.1109/LED.2015.2474817.

[6] K. Nomoto *et al.*, "1.7kV and 0.55mΩ·cm^2 GaN p-n diodes on bulk GaN substrates with avalanche capability," *IEEE Electron Device Lett.*, vol. 37, no. 2, pp. 161–164, Feb. 2016, doi: 10.1109/LED.2015.2506638.

[7] Y. Cao, R. Chu, R. Li, M. Chen, and A. J. Williams, "Improved performance in vertical GaN Schottky diode assisted by AlGaN tunneling barrier," *Appl. Phys. Lett.*, vol. 108, no. 11, pp. 1–5, Mar. 2016, doi: 10.1063/1.4943946.

[8] W. Li *et al.*, "Design and realization of GaN trench junction-barrier-Schottky-diodes," *IEEE Trans. Electron Devices*, vol. 64, no. 4, pp. 1635–1641, Apr. 2017, doi: 10.1109/TED.2017.2662702.

[9] S. W. Han, S. Yang, and K. Sheng, "High-voltage and high I_{ON}/I_{OFF} vertical GaN-on-GaN Schottky barrier diode with nitridation-based termination," *IEEE Electron Device Lett.*, vol. 39, no. 4, pp. 572–575, Apr. 2018, doi: 10.1109/LED.2018.2808684.

[10] Y. Zhang *et al.*, "Novel GaN trench MIS barrier Schottky rectifiers with implanted field rings," in *IEEE Int. Electron Devices Meeting Tech. Dig. (IEDM)*, San Francisco, CA, USA, Dec. 2016, pp. 1–4, doi: 10.1109/IEDM.2016.7838386.

[11] A. D. Koehler *et al.*, "Vertical GaN junction barrier Schottky diodes," *ECS J. Solid State Sci. Technol.*, vol. 6, no. 1, pp. Q10–Q12, Jan. 2017, doi: 10.1149/2.0041701jss.

[12] Y. Zhang *et al.* "Vertical GaN junction barrier Schottky rectifiers by selective ion implantation," *IEEE Electron Device Lett.*, vol. 38, no. 8, pp. 1097–1100, Aug. 2017, doi: 10.1109/LED.2017.2720689.

[13] Y. Zhang *et al.*, "GaN-on-Si vertical Schottky and p-n diodes," *IEEE Electron Device Lett.*, vol. 35, no. 6, pp. 618–620, Jun. 2014, doi: 10.1109/LED.2014.2314637.

[14] Y. Wang *et al.*, "Ultra-low leakage and high breakdown Schottky diodes fabricated on free-standing GaN substrate," *Semicond. Sci. Technol*. vol. 26, no. 2, pp. 1–4, Dec. 2011, doi: 10.1088/0268-1242/26/2/022002.

[15] S. Hashimoto, Y. Yoshizumi, T. Tanabe, and M. Kiyama, "High-purity GaN epitaxial layers for power devices on low-dislocation-density GaN substrates," *J. Cryst. Growth*, vol. 298, pp. 871–874, Jan. 2007, doi: 10.1016/j.jcrysgro.2006.10.117.

[16] N. Tanaka, K. Hasegawa, K. Yasunishi, N. Murakami, and T. Oka, "50 A vertical GaN Schottky barrier diode on a free-standing GaN substrate with blocking voltage of 790 V," *Appl. Phys. Exp.*, vol. 8, no. 7, pp. 1–3, Jun. 2015, doi: 10.7567/APEX.8.071001.

[17] D. Disney, H. Nie, A. Edwards, D. Bour, H. Shah, and I. C. Kizilyalli, "Vertical power diodes in bulk GaN," in *Proc. Int. Symp. Power Semicond. Devices IC's*, Kanazawa, Japan, May 2013, pp. 59–62, doi: 10.1109/ISPSD.2013.6694455.

[18] Y. Saitoh *et al.*, "Extremely low on-resistance and high breakdown voltage observed in vertical GaN Schottky barrier diodes with high-mobility drift layers on low dislocation-density GaN substrates," *Appl. Phys. Exp.*, vol. 3, no. 8, pp. 1–3, Jul. 2010, doi: 10.1143/APEX.3.081001.

[19] X. K. Liu *et al.*, "1.2 kV GaN Schottky barrier diodes on free-standing GaN wafer using a CMOS-compatible contact material," *Jpn. J. Appl. Phys.*, vol. 56, no. 2, pp. 1–5, Jan. 2017, doi: 10.7567/JJAP.56.026501.

[20] S. W. Han, S. Yang, and K. Sheng, "Fluorine-implanted termination for vertical GaN Schottky rectifier with high blocking voltage and low forward voltage drop," *IEEE Electron Device Lett.*, vol. 40, no. 7, pp. 1040–1043, Jul. 2019, doi: 10.1109/LED.2019.2915578.